International Journal of Thermophysics, Vol. 17, No. 5, 1996

Density Measurements on Levitated Liquid Metal Droplets[1]

E. Gorges,[2,3] L. M. Racz,[4] A. Schillings,[2] and I. Egry[2]

Electromagnetic levitation is a useful tool for measuring thermophysical properties of high-temperature melts such as liquid metals. Due to its noncontact nature, the undercooled regime is also accessible. Density and thermal expansion of a levitated drop can be derived from volume measurements, if its mass is known. Assuming cylindrical symmetry, the volume of a drop can be determined from its cross section. Using photography, such measurements on liquid metals have been performed in the past. Here we present an improvement of this method, which replaces the photographic camera with a CCD videocamera and subsequent digital image processing. This reduces the time effect required to obtain the results and allows one to average over disturbing surface oscillations. The specific problems of digital image processing, namely resolution and edge detection, are addressed and results on nickel are presented.

KEY WORDS: density; image processing; levitation; liquid metals; nickel; undercooled melt.

1. INTRODUCTION

Density is an important thermophysical property of liquid metals in materials science, casting processes, and hydrodynamics. Because of the high temperatures and the chemical reactivity of the samples, measurements of properties are difficult in general. The levitation technique is a very elegant way to overcome most of these problems [1].

[1] Paper presented at the Fourth International Workshop on Subsecond Thermophysics, June 27–29, 1995, Köln, Germany.

[2] Institute for Space Simulation, German Aerospace Establishment (DLR), D-51147 Köln, Germany.

[3] To whom correspondence should be addressed.

[4] Humboldt fellow. Permanent address: Department of Mechanical Engineering, Tufts University, Medford, Massachusetts 02155, U.S.A.

0195-928X/96/0900-1163$09.50/0

The droplet is observed by a CCD camera and the video sequences are evaluated by an image processing system. If we are able to measure the volume, we can calculate the temperature dependent density by

$$\rho(T) = \frac{M}{V(T)} \tag{1}$$

One of the advantages of our technique is the large temperature range ($T = 1000$–$2000°C$) within which density measurements can be made. It is possible to obtain density values even in the undercooled state and the data can be quickly evaluated. Typically, the thermal expansion coefficient

$$\alpha = \frac{1}{V}\frac{\partial V}{\partial T} \tag{2}$$

is of the order of 10^{-5}–10^{-4} which defines the requirement on the resolution of our method.

2. EXPERIMENTAL ARRANGEMENT

Figure 1 shows a schematic diagram of the levitation facility at DLR in Köln. The whole process takes place inside a chamber, which can be

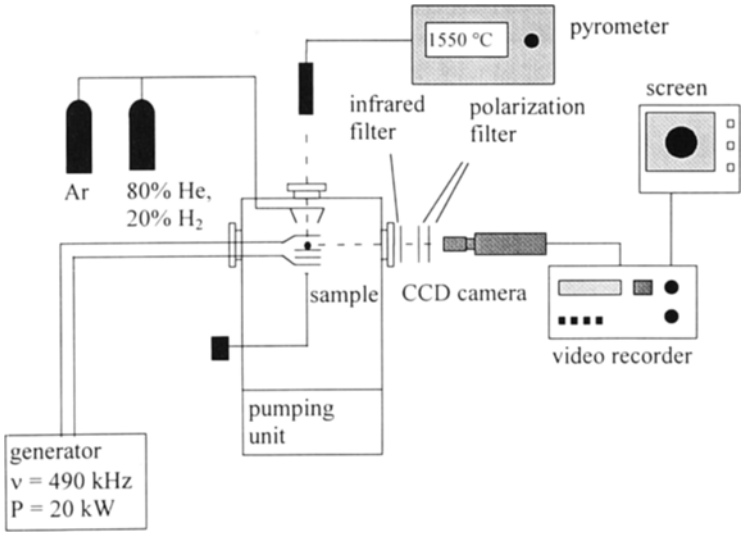

Fig. 1. Experimental arrangemant of the DLR levitation system with gas supply, CCD camera/VCR unit, and pyrometer.

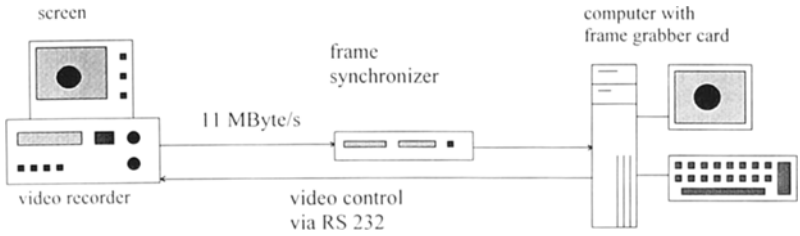

Fig. 2. Schematic diagram of the image processing system, containing a VCR, a frame synchronizer, and a PC with a frame grabber card.

evacuated to a pressure of 10^{-6} mbar and back filled with an inert gas or with a He–H_2 mixture to provide a reducing atmosphere.

An electric current through the coil generates an electromagnetic field which induces currents in the sample. The result is a Lorentz force, acting on the sample and compensating the gravitational force. The sample levitates without any contact with the crucible. Due to the resistivity of the material, the sample heats up and melts. The temperature of the sample is controlled by the gas flow and measured with a pyrometer. During the levitation, video sequences are taken by the CCD camera and stored on a standard S-VHS VCR (videocassette recorder).

The brightness of the pictures changes with temperature. The intensity falling on the camera is kept constant by controlling the angle between two polarization filters. The camera has its maximum sensitivity in the infrared domain. The polarization filters work only in the visible region. For this reason, we use an infrared filter with a very low transmission rate in the infrared wavelength regime (starting from 1 μm).

The pictures have to be evaluated by a computer. For this reason, the sequences have to be digitized, so that the computer can handle them. Figure 2 shows the hardware of our image processing system. It consits of a VCR and a computer with a frame grabber card. Because of the large amount of data (11 MByte $\cdot s^{-1}$), it is possible neither to store the pictures on the computer nor to evaluate them directly. We solved this problem by working in step modus, letting the computer control the VCR. The pictures are summed up to a level of 100 to 200 pictures, depending on the movement of the surface of the sample. After each frame, an impulse is given to the VCR to move to the next picture. This sum-picture has to be evaluated further.

3. IMAGE PROCESSING

A simple and fast method to obtain the cross section of the sample consists in binarizing the obtained images by setting a threshold value for

the intensity. The change from black to white, and vice versa, defines the edge within pixel resolution. The shape of the droplet is than obtained by fitting these data points by a series expansion in Legendre polynomials

$$r(\cos(\vartheta)) = r(u) = \sum_l \varepsilon_l P^l(u) \tag{3}$$

as described in Ref. 2. The volume can be calculated by

$$V = \frac{2\pi}{3} \int_{-1}^{1} du\, r^3(u) \tag{4}$$

Figure 3 shows the results on nickel based on the application of this method. Our data are in good agreement with those due to Shiraishi and Ward [3]. However, the accuracy is not sufficient for a precise determination of the thermal expansion. Consequently, the temperature T_ρ at which the liquid density equals that of the solid cannot be defined. We believe that this is due to the applied image processing, i.e., the use of a threshold for edge detection. In the following section, we present an improved algorithm for edge detection.

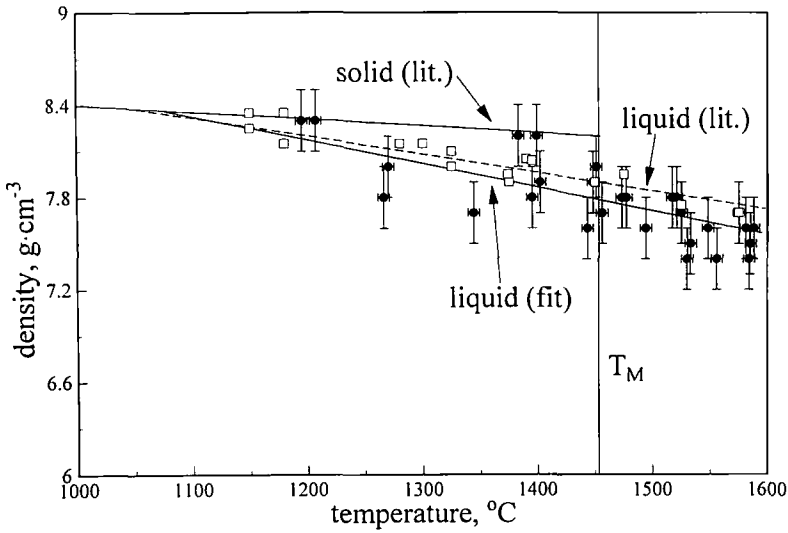

Fig. 3. Density of nickel in the liquid and solid states. Density of solid, taken from Ref. 4. The dashed line is a fit to the data of Shiraishi and Ward [3] (open squares). The full line is a fit to our data (filled circles with error bars).

4. EDGE DETECTION

The sample itself has a sharp edge. The picture of the sample, taken by the CCD camera, is fuzzy due to several effects. First, there is a noisy background in the signal of the different elements of the CCD chip. The blooming effect gives a smearing-out of the picture. One has the sample movement, which gives the same effect. There are also errors resulting from the transmission of the signal through wires and its storage on a VCR, but they are small compared to the other errors. Figure 4 shows such a picture. One can see a single frame with a dark background and a bright spot, representing the cross section of the sample.

Figure 5 shows an intensity profile along a horizontal line, consisting of 768 pixels. The distance between the minimum and the maximum value is of the order of 5–10 pixels and has the same magnitude as the change of length due to temperature changes. For this reason, we discuss the problem of fuzzy pictures. For simplicity, we consider the problem in one dimension.

A very general approach to investigate these effects is to express them by a convolution with a function $g(x)$, representing the fuzziness of the system. The intensity can be calculated by a convolution integral

$$I(x) = \int_{-\infty}^{\infty} dx'\, \tilde{I}(x')\, g(x' - x) \tag{5}$$

$$= \int_{-\infty}^{\infty} dx'\, \Theta(x')\, g(x' - x) \tag{6}$$

where $\tilde{I}(x) = \Theta(x)$ is the step function. Our measurements indicate that the function $g(x)$ is sharply peaked at $x = 0$ and an even function. Evaluating this gives

$$I(x) = \int_{-\infty}^{0} dx'\, g(x' - x) \tag{7}$$

$$= \int_{-\infty}^{x} dx'\, g(x') \tag{8}$$

Calculating the first derivative yields

$$I'(x) = g(x) \tag{9}$$

One can see that the real edge of the picture is given by the maximum of the first derivative of the intensity profile. Figure 6 shows a plot of a step-function, the convolution after Eq. (8), and its first derivative. The maximum of the first derivative gives the position of the edge.

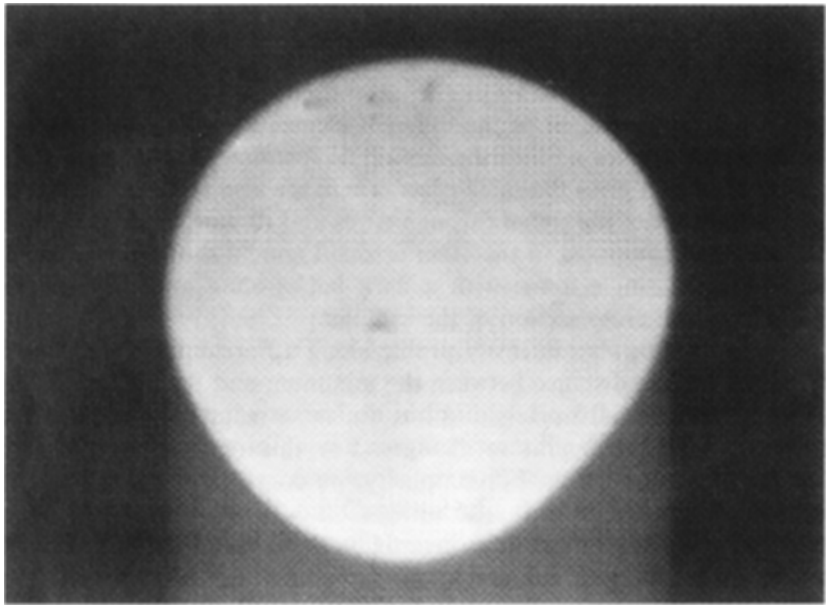

Fig. 4. Original digitized picture of a levitated sample.

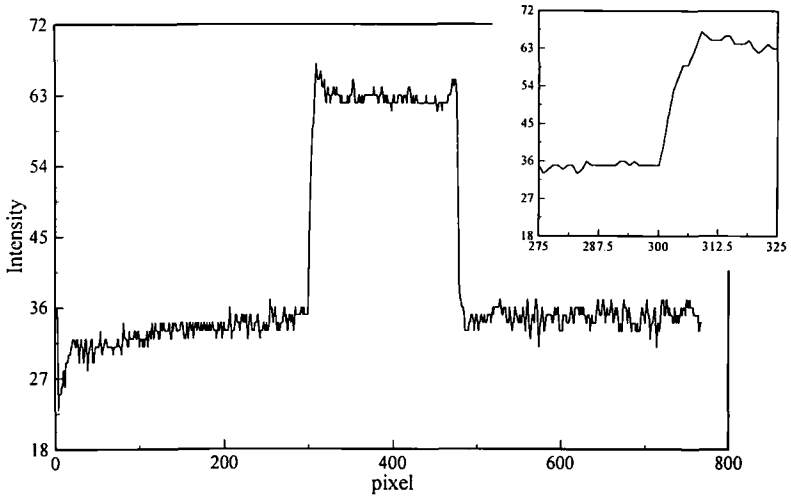

Fig. 5. Cross-sectional intensity profile of the digitized picture, showing its fuzzy edge and the noise.

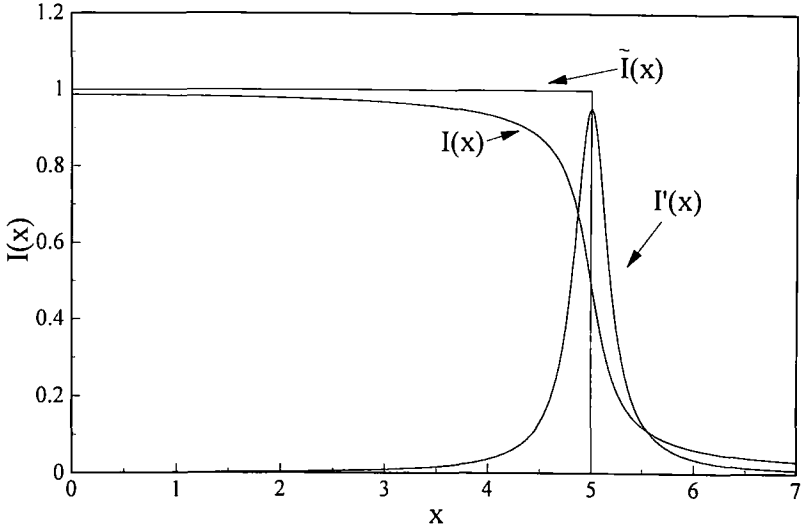

Fig. 6. Original intensity profile, convoluted profile, and its first derivative.

An additional smearing effect arises from the movement of the sample's center of mass and surface. First, we can eliminate any translational movement by working in a coordinate system which is fixed to the center of mass of the sample. The second movement is the oscillation of the surface. It can be expressed as

$$r(\vartheta, \varphi, t) = R(\vartheta) + \xi(\vartheta, \varphi, t) \tag{10}$$

where we use the fact that the static shape of the sample is axially symmetric. The first part of Eq. (10), $R(\vartheta)$, gives the volume. The time-dependent part can be eliminated by averaging. Another advantage of the averaging process is a reduction of noise. Once again, we investigate the one-dimensional case.

Considering an oscillating edge at position

$$r(t) = R_0 + \xi(t) \tag{11}$$

with $\xi(t) = -\delta r \cos(\omega t)$ and $\omega = 2\pi/T$. This yields, in general, for the intensity profile of the picture taken by the camera,

$$I(x) = \lim_{t_0 \to \infty} \frac{1}{t_0} \int_0^{t_0} dt\, \tilde{I}(r(t) - x) \tag{12}$$

This integral can be evaluated as

$$I(x) = \lim_{t_0 \to \infty} \frac{1}{t_0} \int_0^{t_0} dt\, \tilde{I}(r(t) - x) \tag{13}$$

$$= 2 \lim_{N \to \infty} \frac{1}{NT} N \int_0^{T/2} dt\, \tilde{I}(r(t) - x) \tag{14}$$

$$= \frac{2}{T} \int_0^{T/2} dt\, \tilde{I}(r(t) - x) \tag{15}$$

where we use the periodicity of Eq. (11). Taking

$$\frac{dr}{dt} = \delta r \omega \sqrt{1 - \left(\frac{r(t) - R_0}{\delta r} \right)^2} \tag{16}$$

we obtain

$$I(x) = \frac{1}{\pi} \int_{-1}^{1} du \frac{1}{\sqrt{1 - u^2}} \tilde{I}(u - a(x)) \tag{17}$$

with

$$a(x) = \frac{x - R_0}{\delta r} \tag{18}$$

The intesity of the original picture is given by

$$\tilde{I}(x, t) = \Theta(r(t - x)) \tag{19}$$

This results (for $-1 < a < 1$) in

$$I(x) = \frac{1}{\pi} \int_{-1}^{a(x)} du \frac{1}{\sqrt{1 - u^2}} \tag{20}$$

$$= \frac{1}{2} - \frac{1}{\pi} \arcsin(a(x)) \tag{21}$$

which gives

$$I(x) = \begin{cases} 1 & a < -1 \\ \frac{1}{2} - \frac{1}{\pi} \arcsin(a(x)) & -1 < a < 1 \\ 0 & a > 1 \end{cases} \tag{22}$$

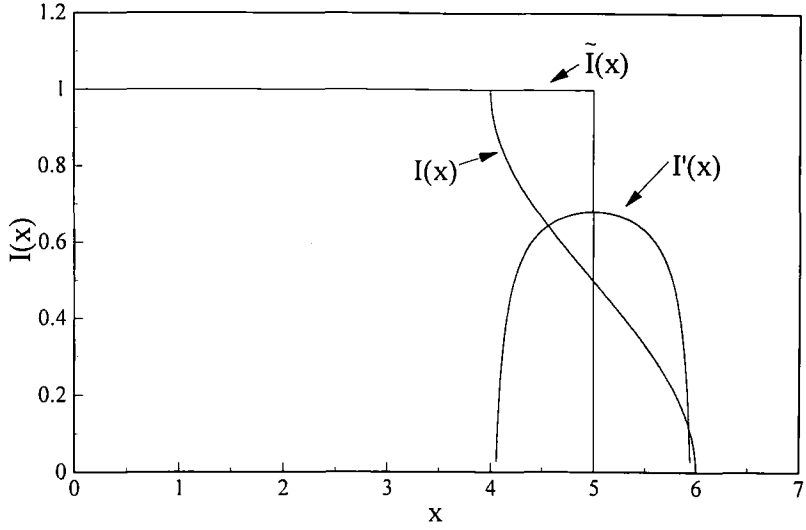

Fig. 7. Original intensity profile, time-averaged profile, and its derivative.

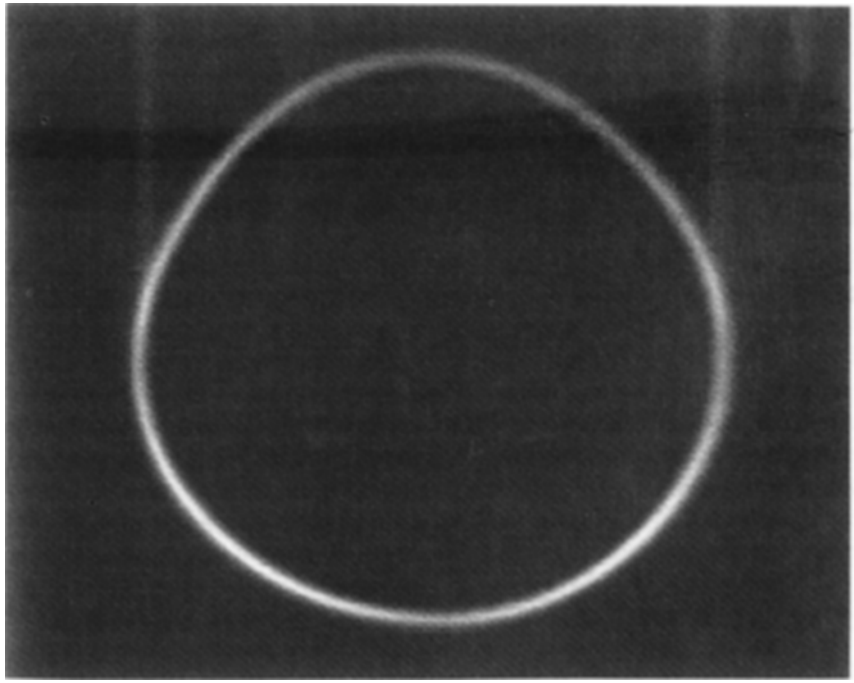

Fig. 8. Edge detection of a moving sample. The average of 100 frames and the first derivative in the radial direction is taken.

For the time-averaged edge, we obtain a form, shown in Fig. 7. The real edge can be calculated from the averaged picture once again by calculating extreme values of the first derivative of the intensity profile.

The problem of detecting the edge has been reduced to the problem of finding the turning points of the curves. Figure 8 is the result of our image processing scheme, which implements the above algorithm. First, we have summed over typically 100 pictures which gives an intensity profile according to Eq. (22). Second, we have applied a radial derivative to find the maximum in intensity as a function of the radius r.

Setting a threshold, the average of the outer and inner line of this picture gives the edge. Doing a least-squares fit with Legendre polynomials [Eq. (3)] on these data points gives the volume according to Eq. (4). It yields the volume in pixel units. A reference picture for calibration is taken of two thin lines at a constant distance.

5. RESULTS AND CONCLUSIONS

We have presented a method for measuring the density of levitated droplets using a CCD camera and image processing. First results on undercooled nickel were obtained which show a good agreement with results previously published. An improved algorithm for edge detection was also presented. This new algorithm has not yet been applied to measurements. They are planned for systems with a high undercoolability such as CoPd, with the goal of approaching the temperature T_ρ at which the densities of solid and liquid states become equal. This should coincide with the glass transition temperature.

REFERENCES

1. D. M. Herlach, R. F. Cochrane, I. Egry, H. J. Fecht, and A. L. Greer, *Int. Mat. Rev.* **38**:273 (1993).
2. L. M. Racz and I. Egry, *Rev. Sci. Instrum.* **66**:4254 (1995).
3. S. Y. Shiraishi and R. G. Ward, *Can. Metall. Q.* **3**:117 (1964).
4. E. A. Brandes, *Smithells Metals Reference Book* (Butterworths, London, 1983).